***Problems of Tribology**, V. 29, No 4/114-2024, 14-23*

Problems of Tribology
Website: http://tribology.khnu.km.ua/index.php/ProbTrib
E-mail: tribosenator@gmail.com

DOI: https://doi.org/10.31891/2079-1372-2024-114-4-14-23

Leakage and rotordynamic coefficients of labyrinth-scallop seals

V. Izemenko, A. Zahorulko*, Yu. Zahorulko

Sumy State University, Ukraine
**E-mail: a.zagorulko@cm.sumdu.edu.ua*

Received: 15 September 2024: Revised: 30 September 2024: Accept: 15 October 2024

Abstract

Reducing leakages and improving the rotor-dynamic damping characteristics of annular seals is an essential problem of sealing technology. A whole range of damping seals are used to seal the shafts of turbomachines, such as honeycomb, hole pattern, pocket, and scallop seals. To reduce the cost and production time, the scallop seals are increasingly used. They showed quite good dynamic and leakage characteristics in the modernization of compressors in the chemical industry. Some designs of scallop seals are able not only to increase dynamic performance (additional use of swirl brakes in the form of semi-open scallops at the inlet) but also thanks to the hybrid design of the scallop and labyrinth seal made of PEEK material, which ensures a minimum clearance between the seal and the shaft, reduce leakages of pumped fluid.

This paper presents the results of calculating the rotordynamic and flow rate characteristics of scallop and labyrinth-scallop seals depending on the operating parameters using computational fluid dynamics (CFD) methods. The CFD was used to calculate the hydrodynamic and rotordynamic characteristics of the seal with shaft whirl. The rotordynamic coefficients were obtained using the frequency excitation method. The obtained characteristics were compared with experimental data available from the literature for annular and labyrinth seals. The study confirmed the relatively low leakages, the high dynamic characteristics of the labyrinth-scallop seals, and the frequency dependence of the stiffness and damping coefficients. It has been confirmed that sickle-shaped scallops create obstacles to the circumferential flow of the working medium. Reducing the circumferential gas flow increases the hydraulic resistance in the grooves and simultaneously minimizes the circulation forces that create shaft whirl, increasing vibration.

Keywords: leakage, rotordynamic coefficients, labyrinth and scallop seal, damping seal, swirl brakes

Introduction

As is known, leakages in the seals of high-pressure centrifugal compressors are limited due to the use of potential pressure energy to overcome local resistances, frictional resistance along the channel length, and sometimes inertial resistance. The larger leakage, the smaller part of potential energy is transferred to the kinetic energy of the flow, as well as the lower values of the average velocity of the liquid in the channel and its mass flow rate. Thus, annular seals are not completely eliminated, but only limit flow rates.

Labyrinth seals, in which local resistances prevail, can be attributed to seals with throttling channels. The main function of labyrinth seals is to ensure minimal leakage through the sealing surfaces, taking into account minimal aerodynamic effects on the compressor rotor. However, in labyrinth seals, due to the fluid flow in the circumferential direction, while the flow is carried by the rotating shaft, circulating aerodynamic forces arise. Therefore, in practice, a number of annular seals have been proposed, which can reduce circulating forces that cause an increase in rotor whirl and, accordingly, vibration. These basic seals include honeycomb, hole-pattern, pocket and scallop seals. If the sealing mechanism and dynamic characteristics of the first three types of seals are well studied [1-6], a rather limited number of studies and publications are devoted to the last type of seals [7-10].

Scallop seals (Fig. 1. a) are widely used and have proven themselves in the process of modernization of compressors for the chemical industry [8]. There are a number of designs of scallop seals that are able not only to improve dynamic characteristics (Fig. 1. a), but also to reduce leakages of the pumped medium (Fig. 1. b) [8].

The first patent for the scallop seal design (Fig. 2. a, b shows the longitudinal section and the isometric view of the seal) [11,12] was obtained in 1984. And it has a sleeve 1 on the inner surface of which there is scallops 2. In the axial direction, the rows of scallops are separated by ridges 4, and in the circumferential direction, adjacent scallops are separated by bridges 3. The ridges perform the same role as the ridges in conventional labyrinth seals, and the bridges slow down the circumferential flow.

The role of bridges is particularly important because, by slowing down the circumferential flow, they thereby reduce the circulating force, the existence of which is the main reason for the loss of dynamic stability of the rotor in the seals. In addition, the scallops are semi-closed chambers that slow down the expansion flow and, accordingly, increase the damping force [13].

In the research work of A. Gulyi [7] presents the experimentally obtained characteristics of flow rate and stiffness for three types of liquid seals, namely: labyrinth with overlapping ribs, scallop and honeycomb seals. All characteristics were compared with the characteristics of standard annular seals. Flow rates, amplitudes, and phases of forced rotor oscillations were measured at four pressure drop values of 0.2; 0.5; 1.0; 2.0 MPa at rotational speeds from 0 to 1000 s^{-1} in steps of 50 s^{-1}. Leakage rate characteristics of all types of seals, with an averaged rotational frequency, show that the minimum flow rates were obtained for a labyrinth seal with a small axial gap between the ridges. Flow rates throughout scallop, honeycomb and labyrinth seals with central location of ridges are almost the same and about 20% less compared to flow rates due to standard annular seal. Numerical values of hydrostatic stiffness are determined by evaluating parameters based on phase and amplitude-frequency characteristics. The latter applies to all types of seals with a pressure drop value of 1 MPa. The type of characteristic corresponds to the model of the dynamic system of the rotor seal as a linear oscillating system of the second order. The honeycomb seal has more dominant dynamic properties, and the scallop seal is closer to the standard one. If the tasks of reducing vibration and leakage are equally important for a particular pump, then scallop seals should be used. In terms of hydraulic resistance, they are not inferior to labyrinth and honeycomb seals, and in terms of damping and stiffness properties, they significantly exceed them. At the same time, they are less prone to scoring than conventional annular and labyrinth seals. However, it should be remembered that the coefficient of hydrostatic stiffness of scallop seals is approximately two times lower than that of conventional annular seals [13].

Gocha Chochua [9] investigated the flow between the surface of the stator with scallops made by a disk cutter and the smooth surface of the rotor in a scallop seal with sloping sidewalls developed by Dresser-Rand using the Computational Fluid Dynamics (CFD) method. The main direction in the calculation of the scallop seal was the study of the turbulent compression flow under the action of the pressure drop for the periodic region, the assessment of the effect of the rotor rotation and the swirl at the inlet on the physics of the flow, the extrapolation of the results for the periodic region on the full geometry of the seal and determination of friction coefficients due to pressure losses and shear stress.

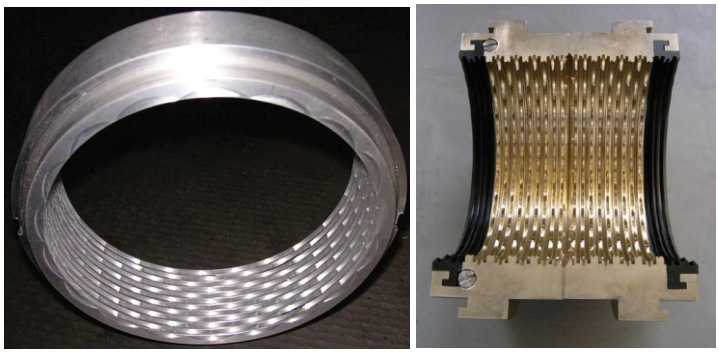

a) b)

Fig. 1. Designs of scallop seals [8]

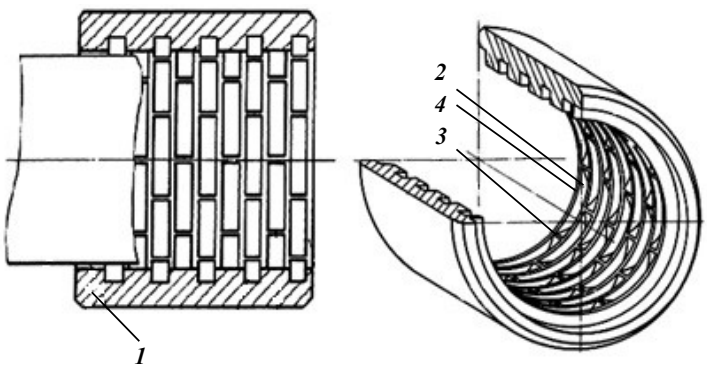

Fig. 2. The first patented design of scallop seal [14]

In his paper, Naohiko Takahashi et al. (Hitachi, Ltd. Company) [10] presented an evaluation of the rotordynamic coefficients of a scallop seal that has elongated ridges and sloping sidewalls with narrow ribs, as in labyrinth seals. The results of the experiment showed that the new seal had improved damping, which is in good agreement with the calculation results based on the bulk flow and CFD analysis by the excitation method. In the analysis by the excitation method, the whirl motion was considered as a stationary problem using a rotating frame of reference. The friction coefficients for the rotor surface, the stator surface, and the surface between the two control volumes for the bulk flow model were determined using steady-state CFD analysis.

The scallop seal can also be made in a stepped configuration, which is used in the unloading piston seals to change the diameter in the axial direction [8,10].

Based on the analysis of previous studies, we can draw the following conclusions and formulate the purpose of this study. Scallop seals showed quite good dynamic and flow rate characteristics during the modernization of compressors in the chemical industry. There are a number of designs of scallop seals that are able not only to increase dynamic performance (additional use of swirl brakes in the form of semi-open scallops at the inlet), but also thanks to the hybrid design of the scallop and labyrinth seal made of PEEK material (Fig. 1. b), which ensures a minimum clearance between the seal and the shaft, leakages of the pumped liquid are reduced. However, a number of studies and publications [7-10] are dedicated to scallop seals and are mainly related to the study of flow physics and the friction coefficient for the analysis of losses in scallop seals with inclined side walls [9], as well as obtaining dynamic coefficients using CFD analysis by the frequency excitation method and the bulk flow method for seal with elongated scallops and inclined sides walls [10]. For scallop seal, there are results regarding leakages and stiffness characteristics only for liquid media [7]. There is no comparison of leakage and dynamic coefficients of scallop seals with other types of labyrinth and annular seals for gas mediums. There is no information about the frequency-dependent dynamic coefficients of labyrinth-scallop seal. Due to the fact that the labyrinth-scallop seal is a damping type of seal, therefore, to obtain frequency-dependent rotordynamic stiffness and damping coefficients, it is advisable to use the calculation method of trajectories, which simulates the gas flow and the movement of the shaft along a given orbit.

1. Geometrical parameters, working and boundary conditions of the labyrinth-scallop seal

The calculation of the leakages in the labyrinth-scallop seal can be performed using CFD modeling in the Ansys CFX software [15]. In Fig. 3 a, an example of a geometry sector created in the Ansys Design Modeler software module is shown, in fig. 3 b mesh of the seal sector with imposed boundary conditions, in Fig. 3 c the complete geometry of the labyrinth-scallop seal. The sector geometry is 1/20 of the full geometry. The geometry of the seal consists of inlet and outlet chambers, periodically repeated along the length of the seal of scallop rows, annular channels, and four labyrinths made of PEEK material. The Ansys Meshing software was used to generate a computationally structured hexa mesh for the generated labyrinth-scallop seal geometry. The number of elements in the clearance was equal to 10 elements. The total size of the mesh was equal to 460,000 elements. The analysis of mesh independence of the model was carried out for four different mesh sizes - 137470, 331860, 460000, 653640 cells. The mesh thickened near the walls to obtain the necessary parameter y^+=30-300 for the corresponding k-ε turbulence model.

Table 1 shows the geometrical dimensions and operating conditions obtained for the shaft diameter, length, clearance, and boundary conditions in the experiment for the hole-pattern seal performed in [14].

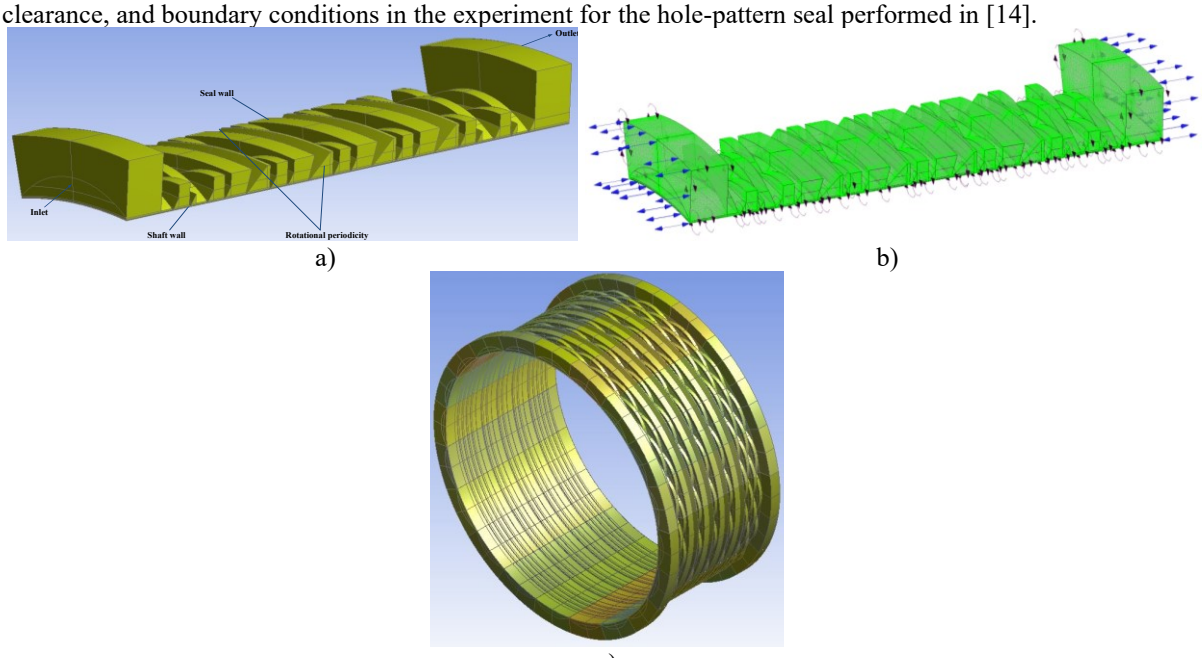

a) b)

c)

Fig. 3. Geometry and boundary conditions of labyrinth-scallop seal

Table 1

Geometrical parameters and operating conditions for scallop seal in CFD modeling

Parameter	Value
Inlet pressure	7.00 MPa
Outlet pressure	3.15 MPa
Inlet temperature	17.4 °C
Shaft rotation speed	20200 rpm
Clearance	0.2 mm
Shaft radius	57.37 mm
Seal length	85.7 mm
Fluid	Air (Ideal gas)
Scallops number in the circumferential direction	20, 30

Calculations were performed using Ansys CFX software which uses a hybrid finite volume method with shape functions from the finite element method to discretize the equations (Reynolds Averaged Navier–Stokes Equations). The k-ε model of turbulence with a standard wall function was used to describe the turbulent flow. The compressibility of a gaseous medium is represented by air as the ideal gas, the total energy equation, and the mass flow balance equation. To check the convergence during the calculation, the mass flow rates at the entrance and exit were monitored. The inlet and outlet boundary conditions were static pressures (Table 1). To take into account the centrifugal and inertial Coriolis forces, the computational domain of the seal was considered in a rotating frame of reference. The shaft wall is in a rotating coordinate system, while the seal wall has a counter-rotating wall boundary condition. This is necessary to create zero velocity with a no-slip wall boundary condition. A static temperature was also set at the seal inlet (Table 1).

3. Mathematical formulation of liquid flow

The averaged Reynolds equations for unsteady simulations, called URANS (Unsteady Reynolds Averaged Navier-Stokes Equations), are given below [15]. In the following equations, the upper underscore is omitted for the averaged values, with the exception of pulsation values

$$\frac{\partial \rho U_i}{\partial t} + \frac{\partial}{\partial x_j}\left(\rho U_i U_j\right) = -\frac{\partial p}{\partial x_i} + \frac{\partial}{\partial x_j}\left(\tau_{ij} - \rho\overline{u_i u_j}\right) + S_M$$

where τ is the molecular stress tensor (which includes both normal and shear stress components). Reynolds stresses $\rho\overline{u_i u_j}$, flow velocities U_i, U_j consist of averaged and pulsational components, ρ is density, S_M is source.

Reynolds-averaged energy equation:

$$\frac{\partial \rho h_{tot}}{\partial t} - \frac{\partial \rho}{\partial t} + \frac{\partial}{\partial x_j}\left(\rho U_j h_{tot}\right) = \frac{\partial}{\partial x_j}\left(\lambda\frac{\partial T}{\partial x_j} - \rho\overline{u_j h}\right) + \frac{\partial}{\partial x_j}\left[U_i\left(\tau_{ij} - \rho\overline{u_i u_j}\right)\right] + S_E$$

The average total enthalpy is given by:

$$h_{tot} = h + \frac{1}{2}U_i U_i + k$$

where h is the specific static enthalpy.

The total enthalpy contains a contribution from the turbulent kinetic energy k:

$$k = \frac{1}{2}\overline{u_i^2}$$

Turbulence models close the averaged Reynolds equations providing the models for calculation, Reynolds stress, and Reynolds fluctuation.

The k-ε model assumes that turbulent viscosity is related to turbulent kinetic energy and turbulent dissipation by the ratio:

$$\mu_t = C_\mu \rho \frac{k^2}{\varepsilon}$$

where C_μ is a constant.

The turbulent kinetic energy k and its dissipation rate ε are derived directly from the differential equations of transfer.

For the ideal gas, the main dependence and equation of state are:

$$dh = c_p(T)dT$$

$$\rho = \frac{p}{RT}$$

where T, p – static temperature and pressure, respectively, c_p– specific heat capacity at constant pressure, R – universal gas constant.

A mixed method of discretization of equations is used. The solution of the system of discretized equations is carried out on the basis of a coupled approach. The pressure and velocity components are determined simultaneously in one cycle.

The most important of the calculations is the calculation of seal mass flow rate. The mass flow through the seal is determined by calculating the following integral on the outlet surface

$$M = \rho U \int_S dA$$

where U is the component of the velocity vector perpendicular to the outlet surface S.

The components of the sealing reaction forces are determined by integrating the pressure field of the sealing medium over the entire shaft surface [14]

$$F_x = -R \int_0^L \int_0^{2\pi} p(\theta, z)\, cos\theta\, d\theta\, dz,\; F_y = -R \int_0^L \int_0^{2\pi} p(\theta, z)\, sin\theta\, d\theta\, dz,$$

where R is the shaft radius, L is the seal length.

4. Results of calculations and comparison of leakages of the labyrinth-scallop seal

As a result of the calculations, the dependences of the mass flow rate through the labyrinth-scallop seal on the pressure ratio $P_r = P_{out} / P_{in}$ and the shaft rotational speed was obtained (Fig. 4). It can be seen from the graphs that with a decrease in the pressure drop and an increase in the rotational speed, the mass flow rate through seal decreases.

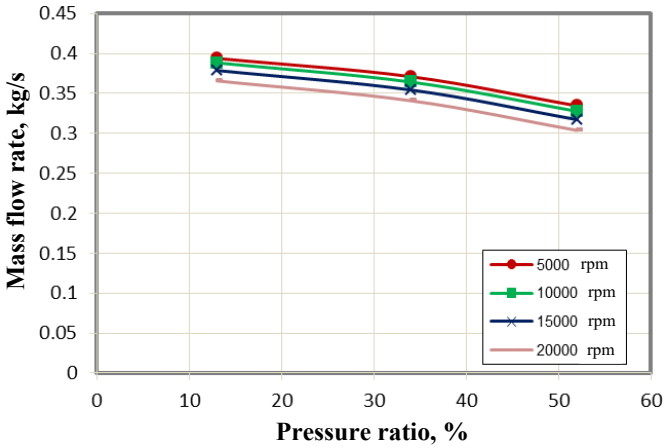

Fig. 4. Dependence of the mass flow rate on the pressure ratio

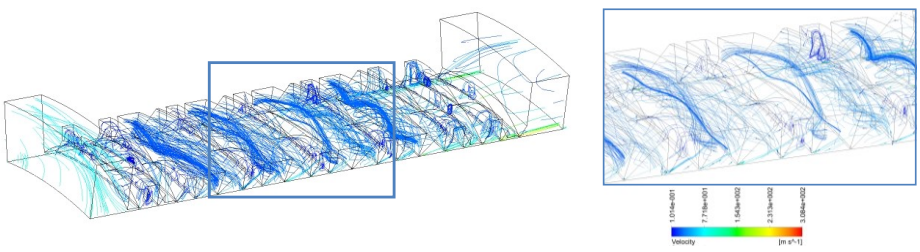

Fig. 5. 3D flow in a labyrinth-scallop seal

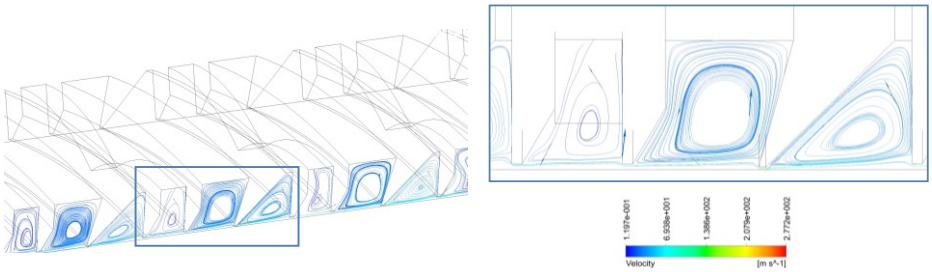

a)

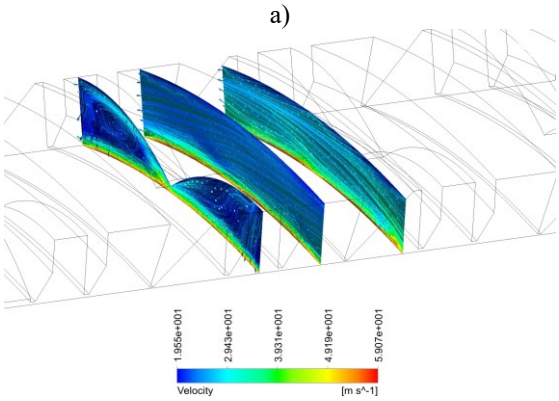

b)

Fig. 6. Vortex flow in the axial (a) and circumferential directions (b)

3D flow in a labyrinth-scallop seal is presented in Figure 5. It has a complex three-dimensional structure with three types of vortex flow, such as circumferential flow in the clearance between the seal and the shaft, vortex flow inside the scallops in the circumferential and axial directions, and vortex flow in the labyrinth annular channel (Fig. 6 a,b).

Fig. 7 a,b shows the field of velocities and pressure in a labyrinth-scallop seal. The distribution of static pressure along the length of the seal (Fig. 8) shows that the largest pressure drop occurs on four labyrinths made of PEEK material with the smallest radial clearance between the seal and the shaft. Moreover, the amplitude of the pressure drop on each subsequent labyrinth increases.

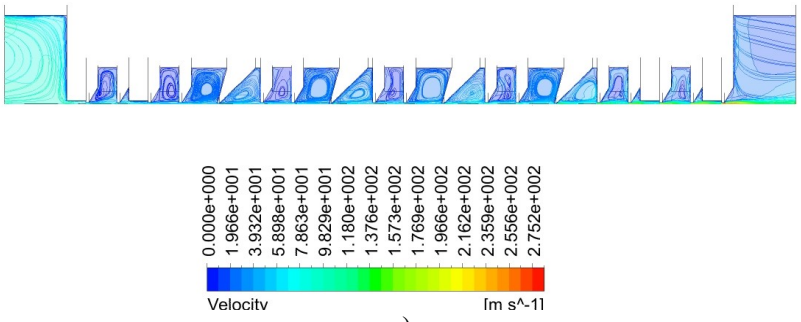

a)

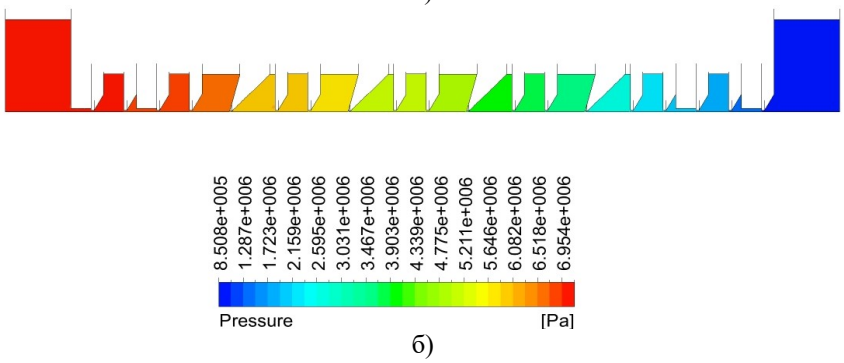

б)

Fig. 7. The velocities (a) and pressure (b) fields

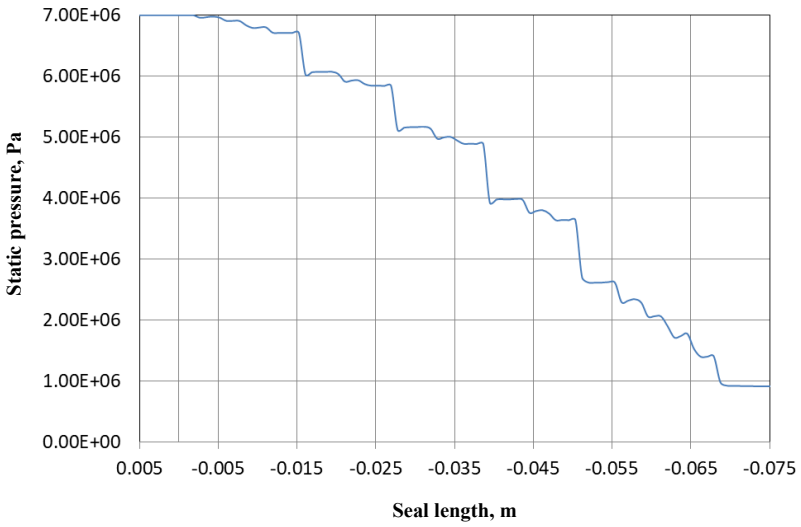

Fig. 8. The static pressure distribution along the seal length

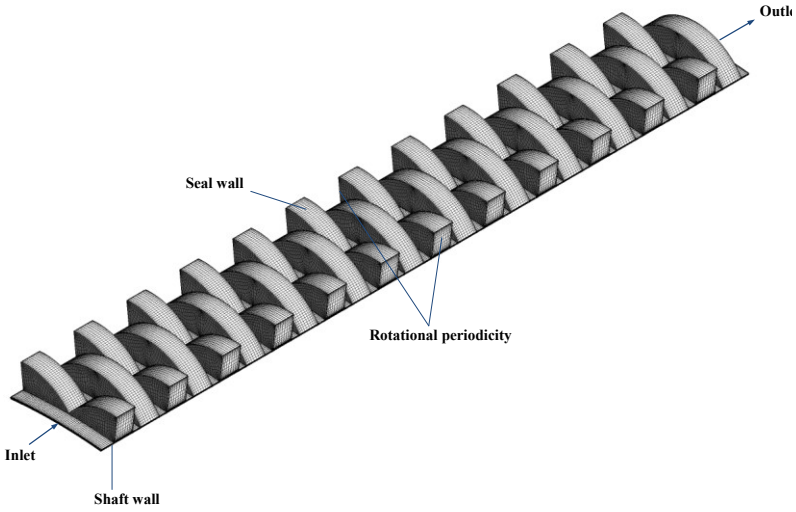

Fig. 9. Calculation mesh and boundary conditions of scallop seal

To compare flow coefficients for annular, labyrinth, scallop, and labyrinth-scallop seals calculations were performed with three different pressure coefficients: $P_r = P_{out} / P_{in} = 0.13,\ 0.34,\ 0.52$. As a scallop seal design, a seal design with 30 crossed rows of scallops was used. An example of the calculation mesh for the scallop seal sector is shown in Fig. 9. The calculation results are presented in a dimensionless form in the form of a flow coefficient [6,16]:

$$\Phi = \frac{M\sqrt{\frac{R_c T_{in}}{2\Delta P P_{in}}}}{\pi D C_r}$$

where M - mass flow rate, R_c - gas constant, P_{in}, T_{in} - pressure and temperature at the inlet, respectively, ΔP - pressure drop at the seal, C_r - radial clearance, D - shaft diameter.

The calculated values were added to the graph obtained by Childs [16] for annular and labyrinth seals (Fig. 1.10). All results are presented at a rotational speed of 10,200 rpm, as this minimizes the effect of rotational speed on the comparison procedure.

It can be seen from Figure 10 that the largest values of the flow coefficient belong to the annular seal, the scallop seal has slightly lower values of the flow coefficient than the traditional labyrinth seal, and the smallest value of the flow coefficient has the labyrinth-scallop seal. Thus, at a pressure ratio of 0.3, the flow coefficient of the labyrinth-scallop seal is 41.7% less than that of the annular seal and 19% less than that of the labyrinth seal.

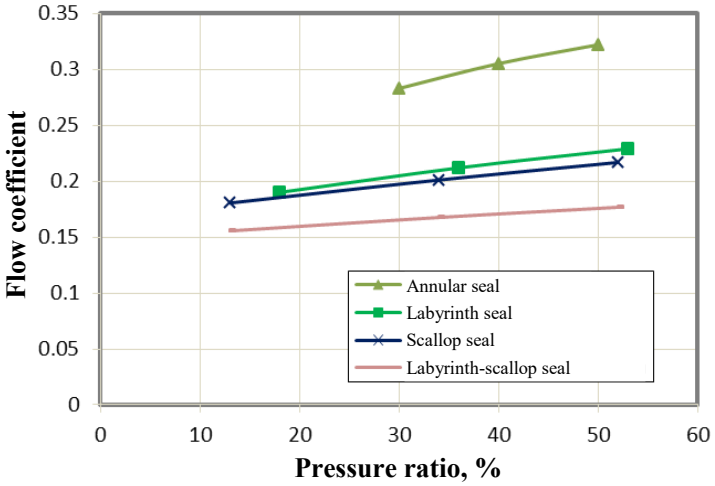

Fig. 10. Dependence of the flow coefficient on the pressure ratio [6,16]

5. Results of comparing the rotordynamic stiffness and damping coefficients of the scallop seal

To calculate the rotordynamic coefficients, a full model of the geometry and mesh of the scallop seal was used. The mesh deformation technology was used to model the shaft uniaxial excitation by the trajectory method. Unsteady calculations were performed for six different frequencies with physical time steps. Depending on the time, the radial and tangential forces of the shaft reaction were obtained, according to which the rotordynamic force coefficients of stiffness and damping were estimated. The amplitude of the shaft movement was 10% of the radial clearance and was equal to 0.02 mm.

To analyze the effectiveness of the scallop seal, it is quite important to compare its rotordynamic force coefficients with the coefficients for other annular seals.

For a more reliable comparison of rotordynamic coefficients, stiffness K and damping C for each seal design, they are presented in the form of normalized coefficients determined by the Childs equation [16]:

$$C^* = \frac{C}{\left(\frac{LD\Delta P}{C_r}\right)}$$

$$K^* = \frac{K}{\left(\frac{LD\Delta P}{C_r}\right)}$$

where L is the seal length, D is the shaft diameter, ΔP is the pressure drop across the seal, and C_r is the radial clearance.

The result of these equations is the normalized damping C^* in seconds, and the normalized stiffness K^*, which is dimensionless (in the graphs presented below, the normalized damping and stiffness values are multiplied by 10^6).

The effective damping coefficient C_{eff} relates the cross-stiffness coefficient k and the direct damping coefficient C and is defined

$$C_{eff} = C(\Omega) - k(\Omega)/\Omega$$

The comparison is made for experimental data obtained for annular and labyrinth seals, which were studied at an inlet pressure of 68.9 bar and various pressure drops. The graphs are taken from the work [6], and the calculated data for the scallop seal are plotted on these graphs (Fig. 11). The graphs (Fig. 11 a,b) show normalized data of effective damping and direct stiffness for labyrinth, annular and scallop seals.

The given dependences show that the traditional labyrinth seal has a negative direct stiffness and very low values of effective damping in the entire range of excitation frequencies. The scallop seal has significantly higher values of direct stiffness and effective damping than the labyrinth seal. However, in the low-frequency range of 40-70 Hz, the effective damping of the scallop seal can take negative values, which can cause loss of shaft stability at these frequencies. The annular seal has more effective damping and comparable stiffness at higher frequencies of 225-300 Hz. Therefore, if the combination of sealing and dynamic stability is important, then a scallop seal should be chosen among the considered types of seals.

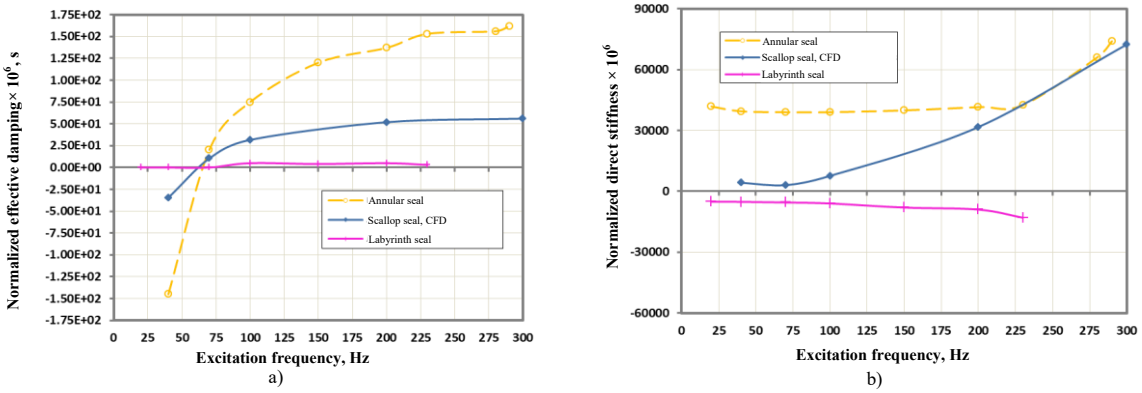

Fig. 11. Comparison of normalized coefficients of effective damping (a) and direct stiffness (b) [6]

Conclusions

Using the repeatedly tested CFD methods for modeling the gas flow in the seal, the values of the labyrinth-scallop leakages and the dynamic characteristics of the scallop seals were obtained. A comparison of the obtained characteristics with experimental data available from the literature for annular and labyrinth seals is given. The study confirmed the rather low values of the labyrinth-scallop leakages and the high dynamic characteristics of the scallop seals, as well as the frequency dependence of the stiffness and damping coefficients.

The study of labyrinth-scallop and scallop seals showed that to improve dynamic characteristics, especially effective damping at low excitation frequencies, it is necessary to use swirl brakes in the form of semi-open scallops at the seal entrance. To reduce leakages, it is advisable to use stepped and hybrid designs of scallop seals, i.e. labyrinth-scallop seals, in which the values of leakages are reduced with sufficiently high dynamic characteristics.

Studies have confirmed that scallops create obstacles to the circumferential flow of the working medium. Reducing the circumferential gas flow increases the hydraulic resistance in the grooves and at the same time reduces the circulation forces that create shaft whirl, increasing vibration. Rows of scallops are characterized by increased strength and rigidity. Scallop seals have good damping properties.

Acknowledgments

This paper was supported by the Sumy State University Projects: Researches on the -Increasing the bearing capacity, sealing and dynamic stability of rotor systems of turbomachines (0123U101853) and -Problems of dynamics and designing of sealing units for centrifugal machines (pumps, compressors) in terms of 4.0 industry (0123U103299) funded by the Ministry of Education and Science of Ukraine.

This research work has been carried out within the project “Fulfillment of tasks of the perspective plan of development of a scientific direction “Technical sciences” Sumy State University” (State Reg. No. 0121U112684) funded by the Ministry of Education and Science of Ukraine.

References

1. Z. Yu, D.W. Childs, A comparison of experimental rotordynamic coefficients and leakage characteristics between hole-pattern gas damper seals and a honeycomb seal, *J. Eng. Gas Turb. Power* 120 (1998) 778-783.

2. D.W. Childs, J. Wade, Rotordynamic-coefficient and leakage characteristics for hole-pattern-stator annular gas seals-measurements versus predictions, *J. Tribol.* 126 (2004) 326-333.

3. M. Vannarsdall, D.W. Childs, Static and rotordynamic characteristics for a new hole-pattern annular gas seal design incorporating larger diameter holes, *J. Eng. Gas Turb. Power* 136 (2014) 022507.

4. B.H. Ertas, Rotordynamic force coefficients of pocket damper seals, Ph.D Dissertation, Texas A&M University, 2005.

5. B. Ertas, A. Gamal, J. Vance, Rotordynamic force coefficients of pocket damper seals, *J. Turbomach.* 128 (2006) 725-737.

6. A.M.G. Eldin, Leakage and rotordynamic effects of pocket damper seals and see-through labyrinth seals, Ph.D Dissertation, Texas A&M University, 2007.

7. A.N. Guliy, Hydrodynamic stiffness of non-contact seals, *Newsl. Mech. Eng.* 2 (1987) 21-25.

8. V. Martsinkovsky, V. Yurko, Economic efficiency of synthesis-gas turbocompressor modernization, *Proc. Eng.* 39 (2012) 339-365.

9. G. Chochua, Computations of gas annular damper seal flows, Ph.D Dissertation, University of Florida, 2002.

10. N. Takahashi, H. Miura, M. Narita, N. Nishijima, Y. Magara, Development of scallop cut type damper seal for centrifugal compressors, *J. Eng. Gas Turb. Power* 137 (2015) 032509.

11. V.V. Usenko, V.A. Martsynkovskyy, I.S. Bereghnoy, A.N. Guliy, Labyrinth seal, Patent SU 1118827 A, 1984.

12. V. Martsynkovskyy, I. Ovseyko, I. Kukharev, Labyrinth seal, Patent UA 20521 U, 2007.

13. V.A. Martsynkovskyy, Rotordynamics of centrifugal machines, SumSU, Sumy, 2012.

14. A. Untaroiu, C. Liu, P.J. Migliorini, H.G. Wood, C.D. Untaroiu, Hole-pattern seals performance evaluation using computational fluid dynamics and design of experiment techniques*, J. Eng. Gas Turb. Power* 136 (2014) 102501.

15. Ansys CFX-Solver Theory Guide, Release 12.1, ANSYS Inc., 2009.

16. D.W. Childs, Bearings+Gas Seals, MEEN 688 Course Presentation, Texas A&M University, 2007.

В. Іземенко, А. Загорулько, Ю. Загорулько. Витоки і ротородинамічні коефіцієнти лабіринтно-лункових ущільнень.

Зменшення витоків і покращення роторно-динамічних демпфуючих характеристик шпаринних ущільнень є важливою задачею ущільнювальної техніки. Для герметизації валів турбомашин використовується цілий ряд демпферних ущільнень, таких як стільникові, з сіткою отворів, кишенькові і лункові ущільнення. Для зменшення вартості і часу виробництва, все частіше використовуються лункові ущільнення. Вони показали досить гарні динамічні та ущільнювальні характеристики при модернізації компресорів хімічної промисловості. Деякі конструкції лункових ущільнень здатні не тільки підвищити динамічні характеристики (додаткове використання вихрових гальм у вигляді напіввідкритих лунок на вході), але й завдяки гібридній конструкції лункового та лабіринтного ущільнень з матеріалу PEEK, яка забезпечує мінімальний зазор між ущільненням і валом, зменшують витоки перекачуваної рідини.

У цій статті наведено результати розрахунку роторно-динамічних і витратних характеристик лункових і лабіринтно-лункових ущільнень в залежності від робочих параметрів за допомогою методів обчислювальної гідродинаміки (ОГД). ОГД методи використовувалися для розрахунку гідродинамічних і ротородинамічних характеристик ущільнення з прецесією вала. Ротодинамічні коефіцієнти отримано методом частотного збудження. Отримані характеристики порівнювали з експериментальними даними, наявними в літературі для шпаринних і лабіринтних ущільнень. Дослідження підтвердило відносно низькі витоки, високі динамічні характеристики лабіринтно-лункових ущільнень, частотну залежність коефіцієнтів жорсткості та демпфування. Підтверджено, що лунки створюють перешкоди для окружного потоку робочого середовища. Зменшення окружного потоку газу збільшує гідравлічний опір у канавках і одночасно мінімізує циркуляційні сили, які створюють прецесію валу, посилюючи вібрацію.

Ключові слова: витоки, ротодинамічні коефіцієнти, лабіринтне та лункове ущільнення, демпферне ущільнення, вихрові гальма